Design of peptide-membrane interactions to modulate single-file water transport through modified gramicidin channels.

Guillem Portella [≠[a]], Tanja Polupanow[#[a]], Florian Zocher[§[a]], Danila A. Boytsov[§], Peter Pohl[§], Ulf Diederichsen[#] and Bert L. de Groot[¶*]

[≠] Institute for Research in Biomedicine - Barcelona
Parc Científic de Barcelona
Baldiri Reixach 10-12, 08028 Barcelona, Spain

[#] Institut für Organische und biomolekulare Chemie
Universität Göttingen
Tammannstr. 2, 37077 Göttingen, Germany

[§] JKU Institute of Biophysics,
Altenberger Strasse 69, A-4040 Linz, Austria

[¶] Computational biomolecular dynamics group,
Max Planck institute for Biophysical Chemistry,
Am Fassberg 11, 37077, Göttingen, Germany
*Corresponding author. E-mail: bgroot@gwdg.de

[a] These authors contributed equally to this work and should be considered as joint first authors.

Table of contents

Supplementary Figures

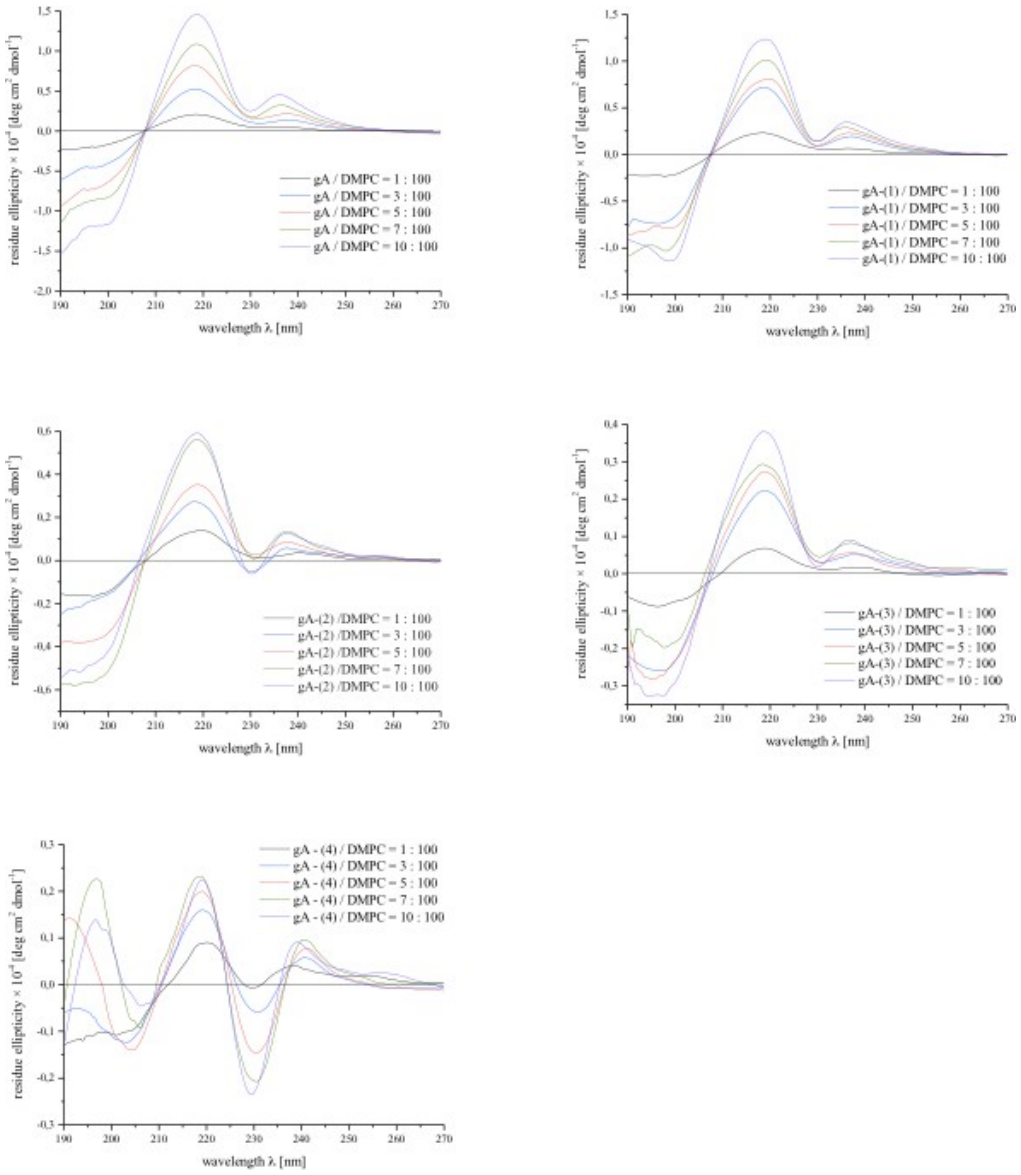

Figure S1. Circular dichroism spectra of gA and its acylated derivatives **gA_1** to **gA_4** into DMPC – vesicles.

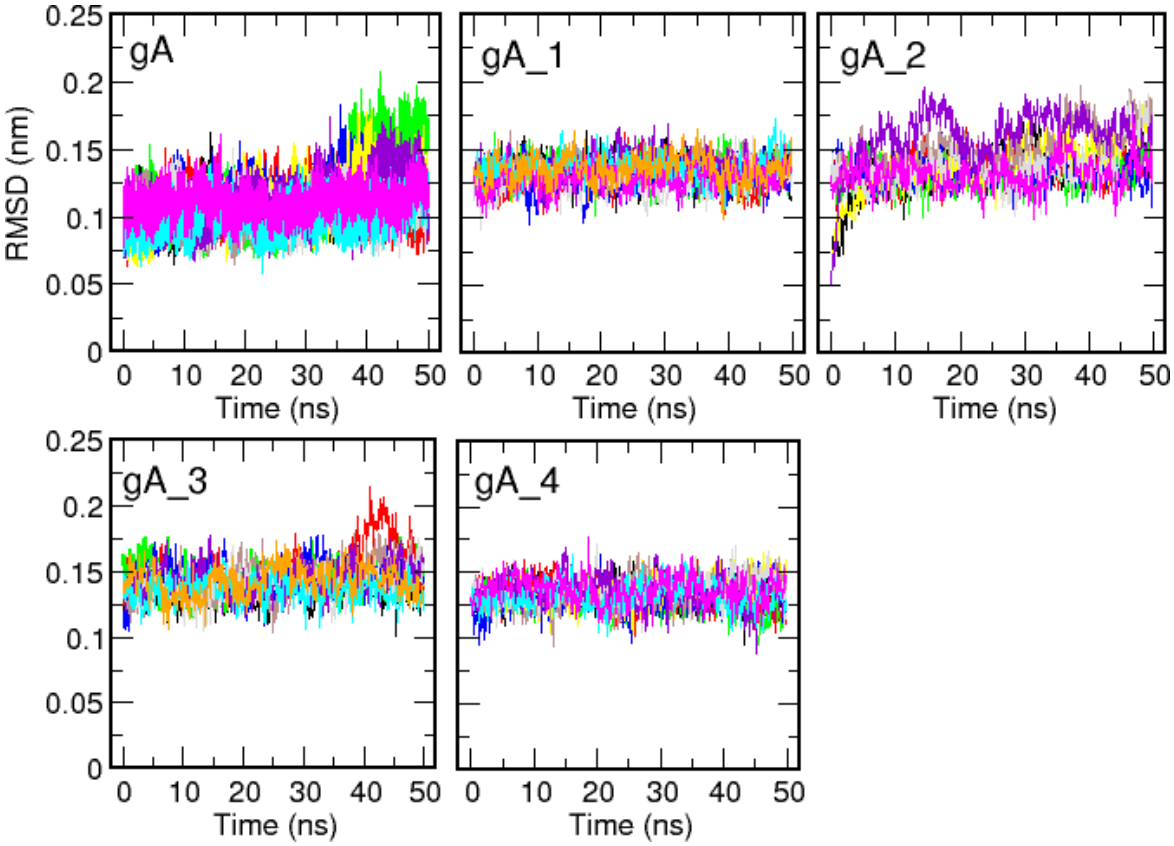

Figure S2. Root mean square fluctuation (RMSD) of the peptide's backbone for each derivative. The reference structure for gA is the force-field minimized NMR structure, for the rest of the derivatives we used the force-field minimized NMR model.

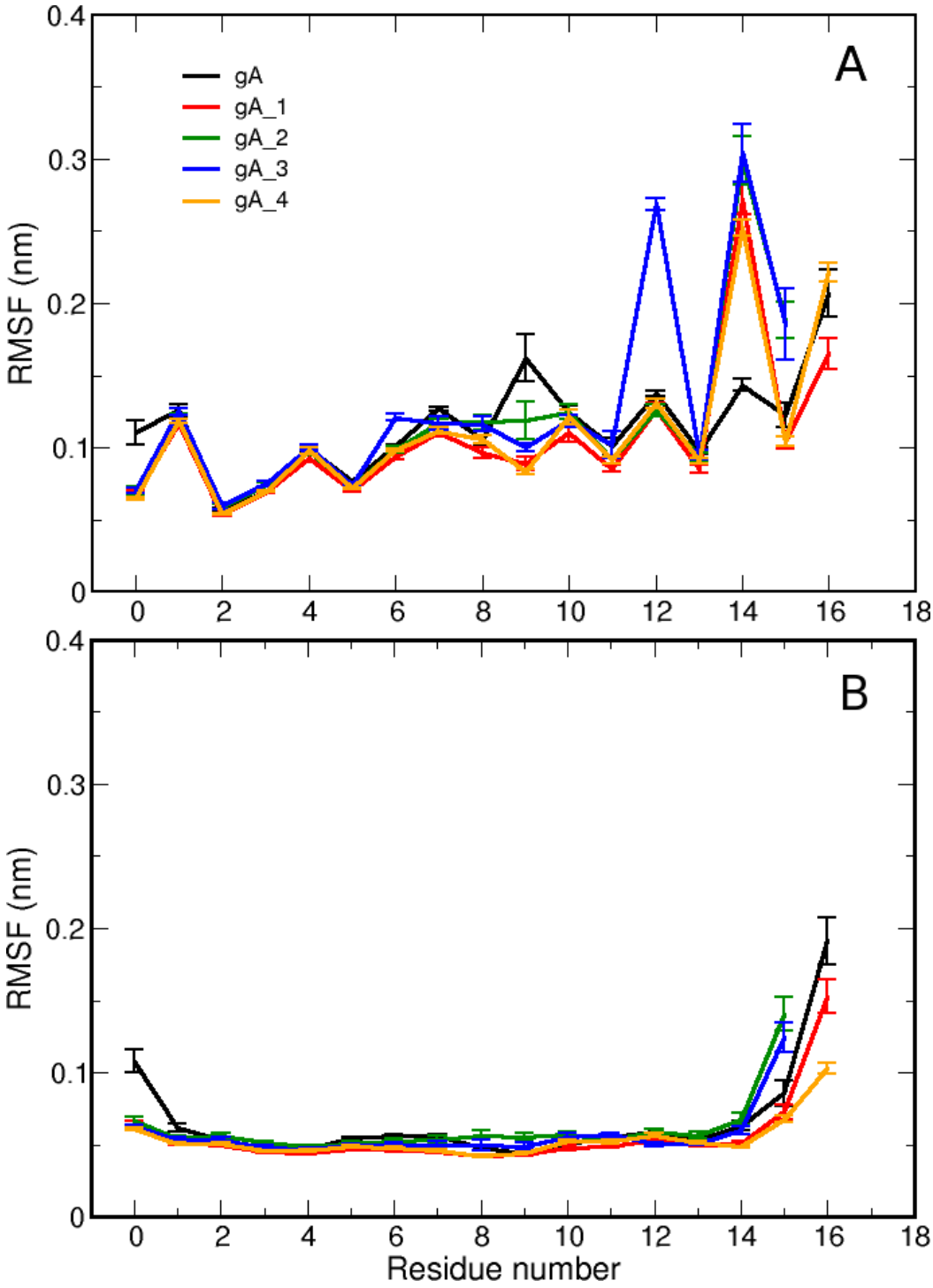

Figure S3. (A) Residue-averaged root mean square fluctuation for gA and their derivatives. Residue number 0 corresponds to the formyl capping group. Notice the large fluctuations at positions occupied by the acyl chains. (B) Residue-averaged backbone root mean square fluctuation (RMSF) for gA and their derivatives. In both graphs, the results are averaged over the two identical monomers.

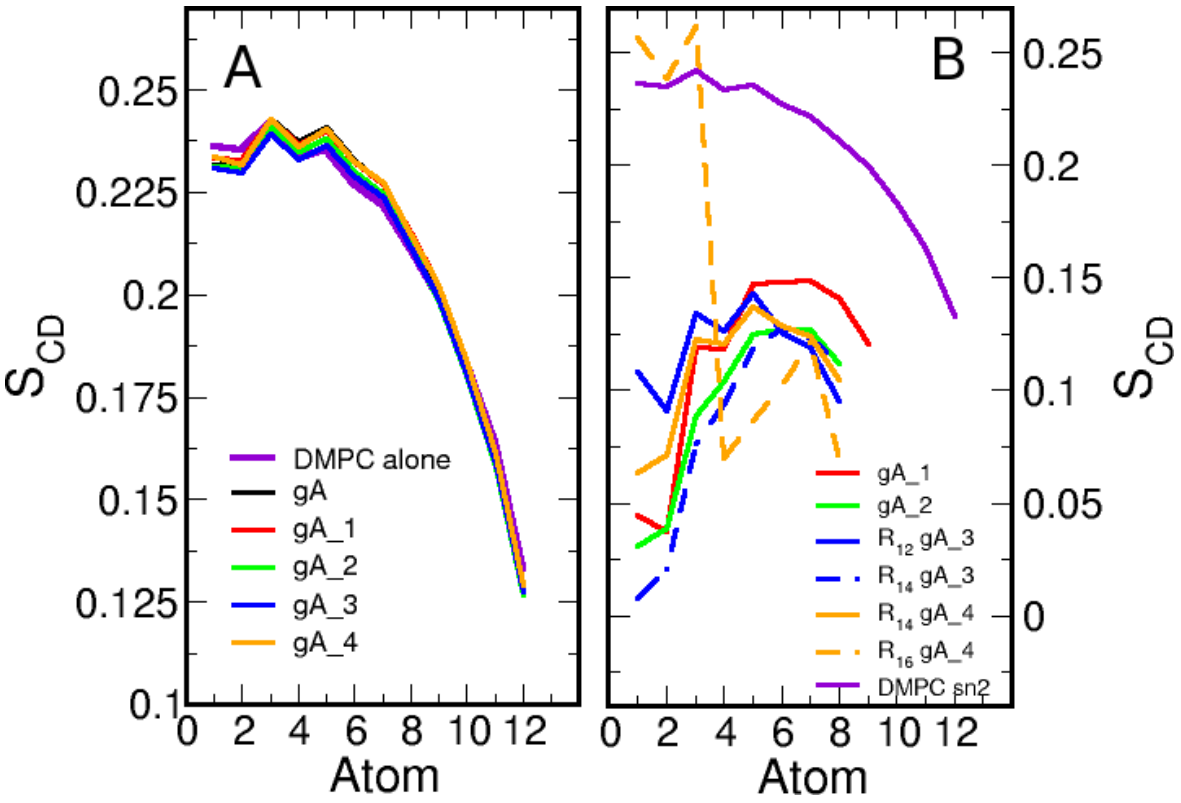

Figure S4. (A) Order parameter S_{CD} as function of the side chain atoms of the sn2 chain of DMPC, as isolated membrane or in the presence of the peptidic channels. (B) Order parameter S_{CD} as function of the side chain atoms of the acylated residues in the new gramicidin derivatives. The Scd order parameter for the sn2 chain atoms of DMPC is included for comparison.

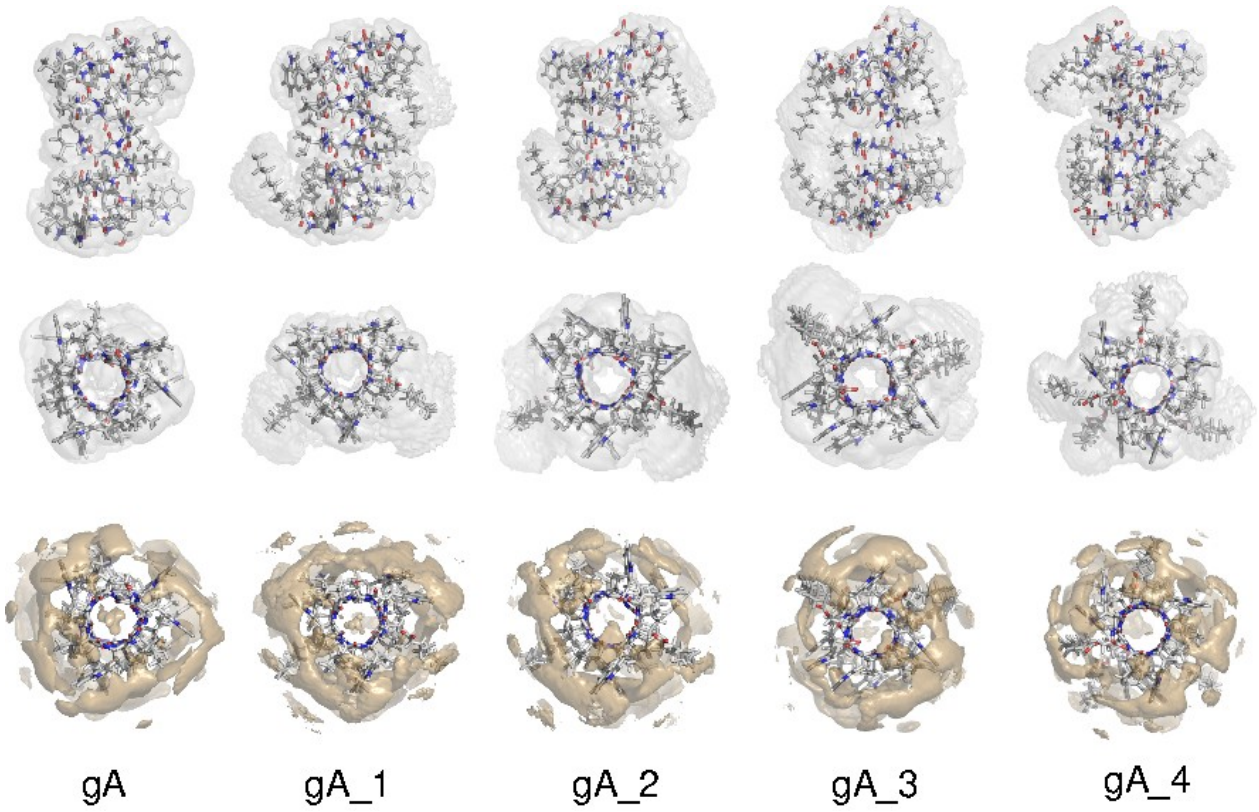

Figure S5. Side (upper row) and top views (lower rows) of the different peptidic channels used in this study. The first two rows depict the peptides surrounded by a peptide density isosurface at a value of 0.5 atoms/nm^3. The lower row shows the density of the lipids that surround the peptidic channels at a value of 2 atoms/nm^3. The data was extracted from our MD simulations.

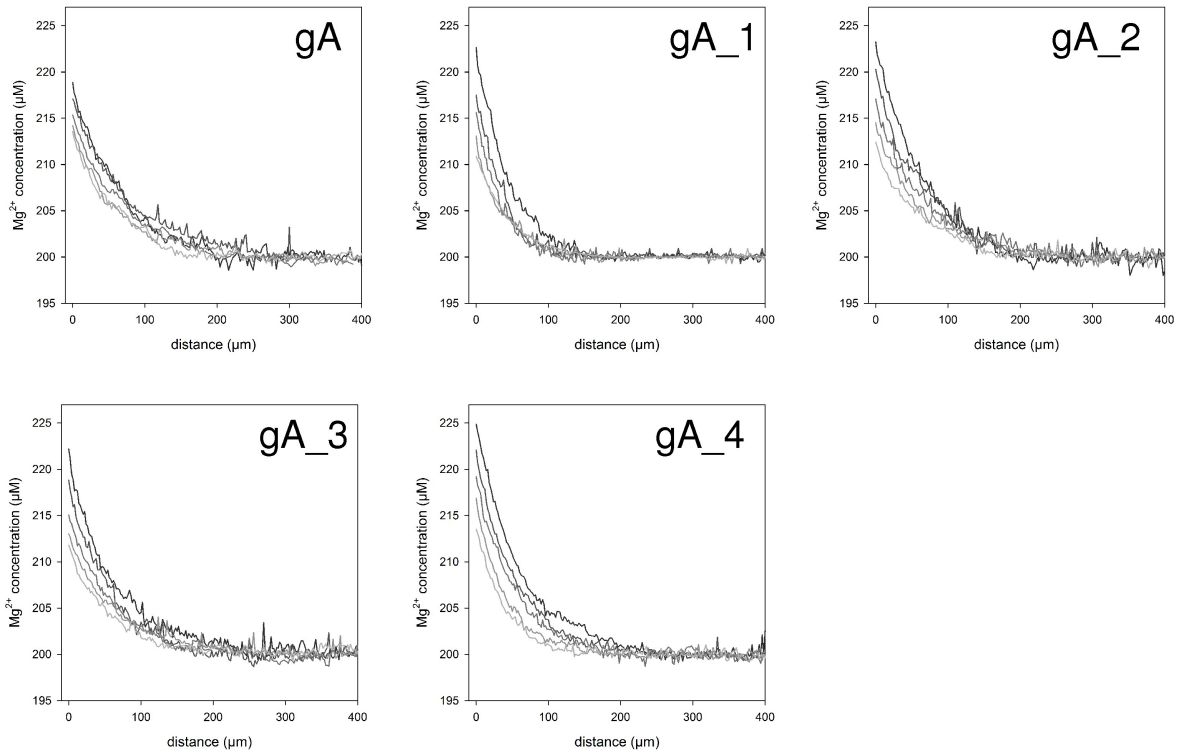

Figure S6. Mg^{2+} concentration profiles in the hypotonic compartment as a function of the distance to the membrane and the peptide concentration. H_2O leaves the compartment but Mg^{2+} cannot follow across the membrane. Consequently, its near-membrane concentration increases. Increasing gramicidin concentration (from light gray to dark gray) resulted in an increasing osmotic water flux. Knowledge of Mg^{2+} concentration distribution allows water flux calculation. The buffer consisted of 150 mM choline chloride, 1 mM potassium chloride, 200 µM magnesium chloride and 20 mM Tris, 1 M urea in the hypertonic compartment, pH 8.4 .

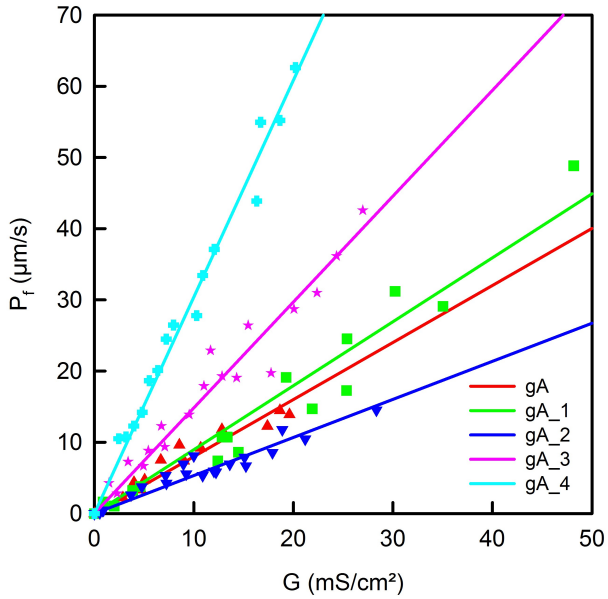

Figure S7. Total membrane water permeability, P_f, as a function of integral electrical membrane conductivity, G. The slope allows calculation of the hydraulic single channel conductances p_f for gA and the gA-derivates (Eq. 2).

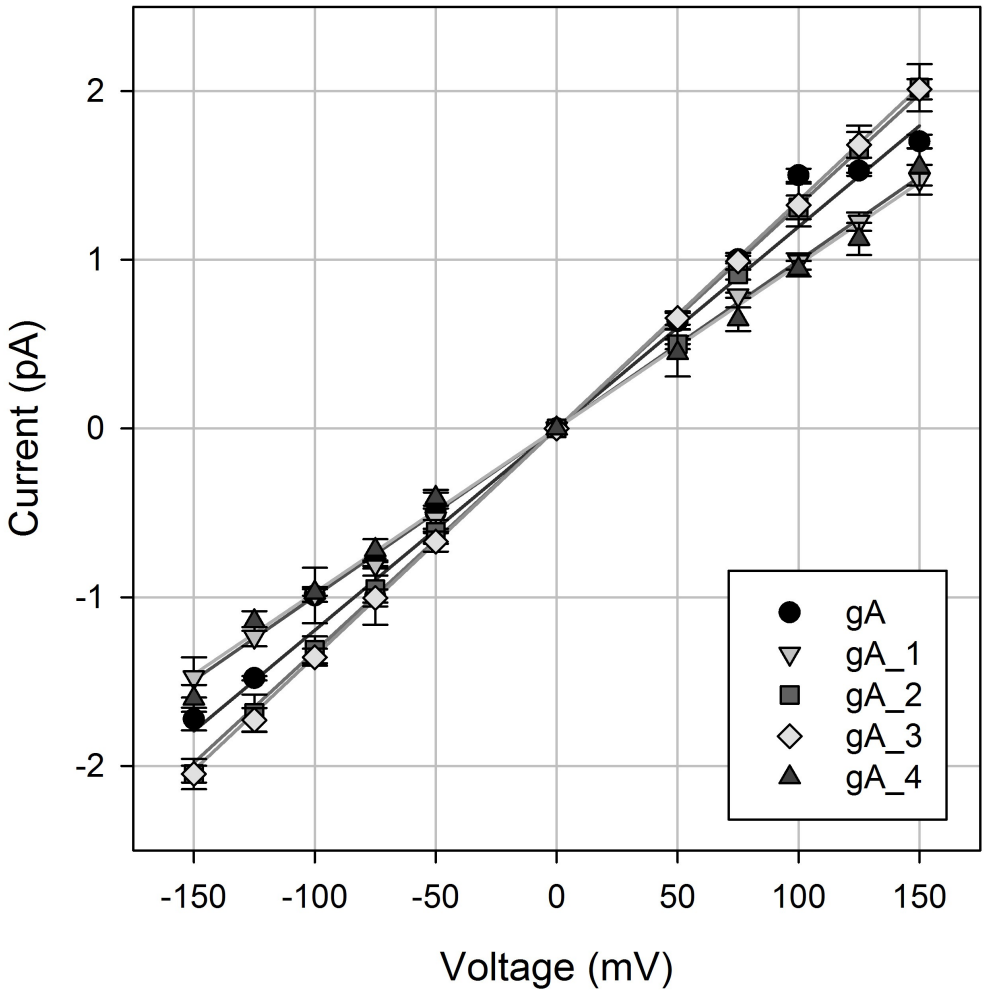

Figure S8. Summary of single channel measurements. We recorded > 100 single channel openings per derivative and voltage. Current histograms of the single events allowed determination of single channel currents. These were then plotted as a function of voltage. The slope of that function indicated the electrical single channel conductance of the particular derivative. The buffer consisted of 150 mM choline chloride, 100 mM KCl, 200 µM $MgCl_2$ and 20 mM Tris, pH 8.4.

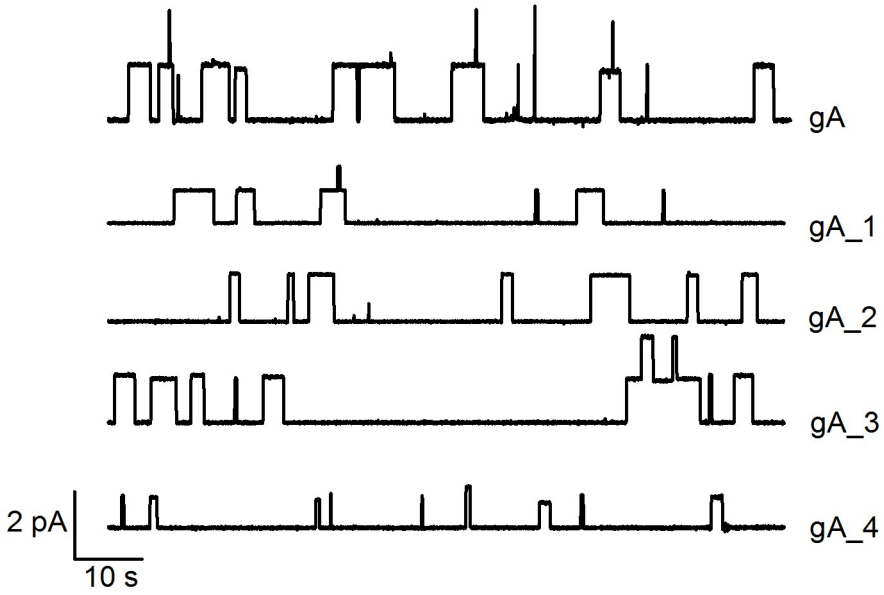

Figure S9. Representative single channel recordings of gramicidin A and its acetylated derivates. Transmembrane voltage was set to 100 mV. The solution contained 100 mM KCl, 150 mM ChCl, 200 µM $MgCl_2$ and 20 mM Tris. The pH was adjusted to 8.4. The recording filter was a 4-pole Bessel with a 3-db corner frequency of 0.1 kHz. Noise reduction was performed by a 12 Hz Gaussian filter .

Supplementary tables

Property	gA	**gA_1**	**gA_2**	**gA_3**	**gA_4**
Mean fully closed / open time fraction per channel (normalized to 1)	0.469 / 0.142	0.399 / 0.145	0.174 / 0.408	0.061 / 0.583	0.022 / 0.607
Mean fully closed / open times per channel (ps)	77 / 35	35 / 20	48 / 70	20 / 65	16 / 59
Mean half open time fraction per channel (normalized to 1)	0.530	0.601	0.826	0.939	0.978
Mean ETA occluding residence time per pore entrance (ps)	140	45	-	-	-
Mean individual lipid head group occluding residence time per pore entrance (ps)	73	72	40	35	32

Table ST1. Pore blockage statistics for the different derivatives used in this study, as extracted from all molecular dynamics simulations using a time resolution of 1ps.

Simulation conditions (membrane and C-terminal charge state)	gA	**gA_1**	**gA_2**	**gA_3**	**gA_4**
DMPC 10 runs of 50ns	1.7 +/-0.5	1.4 +/- 0.4	1.9+/-0.5	1.04+/-0.2	3.9+/-0.4
DPhPC 3 runs of 50ns	2.1 +/- 0.8	3.7 +/- 0.7	1.5 +/- 0.5	0.9 +/- 0.6	3.3 +/-0.4
DPhPC + neutralized terminii 3 runs of 50ns	-	-	-	2.2 +/- 0.2	3.1 +/- 0.5

Table ST2. Computationaly determined osmotic permeability coefficient, in units of 10^{-14} cm^3/s, for gA and its derivatives in DMPC, DPhPC and DPhPC with neutral C-terminal groups. See text for the details on the simulation set-up.

Supplementary Methods

Computational methods

All simulations were carried out using the Gromacs-4 software (1), with periodic boundary conditions and the particle mesh Ewald method (2) for the long-range electrostatics, together with a cut-off of 1.0 nm for the short-range repulsive and attractive dispersion interactions, which were modeled via a Lennard-Jones potential. The Settle algorithm (3) was used to constrain bond lengths and angles of water molecules, and P-Lincs (4) was used for all other bond lengths, allowing a time step of 2fs. The temperature was kept constant at 300 K by using the thermostat method of Bussi et al. (5). The pressure was controlled by coupling the membrane plane and membrane normal independently to a pressure bath of 1 atm (6) .
The force fields for each derivative, including the unmodified gramicidin A, were generated based on the amber99SB parameters. The atomic charges for the modified alkyl residues were derived from standard RESP/6-31G(d) methodology (7), and Lennard-Jones, stretching and bending parameters were generated based on the GAFF force field (8). The force-field parameters for the DMPC and DPhPC molecules was derived from Berger et al. (9) and addapted to correctly interact with the Amber99sb force field (for further details see for example the work of Cordomí et. al (10)). We used the SPC/E (11) model to describe the water molecules. In the case of the peptides without C-termini capping group, two sodium ions (12) were inserted in the water solution to neutralize the system charge.
After an initial minimization, for each system we performed a 10ns equilibration with soft position restraints on the backbone of the peptide derivatives in order to equilibrate the membrane slab around them. The last 2 ns of the position-restrained simulation were used to extract 10 independent structures that were subsequently simulated for 50ns each for the DMPC systems, and 3 sets of 50ns for the derivatives in a DPhPC membrane. We have also performed 3 simulations of 50ns for **gA_3** and **gA_4** in DPhPC with an amino terminal capping group at the C-terminal end of the peptides.
Extraction of the water permeability coefficients was done as previously described (13, 14) using in-house software. Briefly, the osmotic permeability coefficient relates the flux j_w of water molecules between two compartments separated by an osmotic gradient to the difference in osmolite concentration ΔC_s, namely $j_w = p_f \Delta C_s$. In diluted solutions, we can linearly relate the concentration gradient with a difference in chemical potential $\Delta\mu$ between the two compartments,

$$j_w = p_f \left(\Delta\mu / k_B T V_w \right)$$

where V_w is the volume of a water molecule, k_B the Boltzman factor and T the temperature. We can cast the correlated motion of tightly packed column of water inside the channel as an activated process along a collective coordinate that follows the translocation of one water molecule, with an associated activation free energy. In equilibrium the rate of

crossing of such barrier in a given direction is k_0, and it is the same in both directions. In the presence of an osmotic gradient, the free energy of the two states differs by Δμ. Using theory of activated processes one can show (15) that the net molar flux caused by the osmotic gradient can be written as

$$j_w N_A = k_0 \left(e^{\Delta\mu/2\,k_B T} - e^{-\Delta\mu/2\,k_B T} \right) = 2k_0 \sinh\left(\Delta\mu/2\,k_B T \right)$$

Under a linear approximation, we can recast the molar flux as

$$j_w = k_0 \left(\Delta\mu / k_B T N_A \right)$$

From these equations, and considering that the water molar volume is $v_w = V_w / N_A$ the value of the p_f is directly proporitonal to the rate at which the the water column crosses a collective barrier that displaces one water molecule from one compartment to the adjacent one, $p_f = k_0\, v_w$

In our calculations we have counted a transition each time the whole water column moves a typical water-water distance, set to 0.275 nm. From the unidirectional transitions extracted from our MD simulations and using a water molar volume of 0.03 nm^3 we were able to estimate p_f from equilibrium simulations.
Lipid, peptide and water densities were generated using in-house software with a grid of 0.05 nm, associated standard errors were computed from the standard deviations of the 10 independent simulations from each derivative. A lipid head group was considered to be occluding the pore if the positively charged nitrogen was positioned on the pore radius (~0.2nm) and within 1 water molecule distance from it (~0.275 nm). The same threshold was imposed for the heavy atoms of ETA. When the pore entrance is free of lipid head groups or ETA heavy atoms, we consider the pore entrance to be in an open state. RMSD and structure factors were computed using the Gromacs suite of programs. Hydrogen bonding energies were extracted from MD trajectories using the empirical formula of Espinosa *et al.* (16) .

Peptide synthesis and incorporation in the membrane to assess secondary structure

General Remarks. All chemicals were of analytical grade and used without further purification. Solvents were of the highest grade available. Ultra pure water was prepared using the water purification device *Simplicity* (*Millipore*, Bedford, UK). All amino acid derivatives as well as coupling reagents and the resins for solid-phase peptide synthesis were purchased from *NovaBiochem* (Darmstadt, Germany), *IRIS Biotech* (Marktredwitz, Germany), *GL Biochem* (Shanghai, China), *Bachem* (Bubendorf, Switzerland). Methanol (HPLC-grade) was obtained from *FisherScientific GmbH* (Nidderau, Germany). DMPC was obtained from *Avanti Polar Lipids* (Alabama, USA) and gramicidin D from *Fluka* (Taufkirchen, Germany) and purified by silica chromatography using a literature procedure(17) (to afford a final purity of 96 % of gA). CD spectra were recorded on a *Jasco-810A* spectropolarimeter (Gross-Umstadt, Germany) equipped with a *Jasco*

PTC432S temperature controller using the *Jasco Spectra Manager control* (V 1.17.00) and *application* (V 1.53.00) software package. The spectra were recorded at 50 °C in a wavelength range of 270-190 nm with 1.0 nm bandwidth, using 5 mm quartz glass precision cells, 1.0 s response and a scan speed of 50 nm/min. Five spectra were averaged. Spectra were background-corrected against pure vesicle suspensions without incorporated peptides and smoothed (*Savitzky-Golay*). ESI-MS data were obtained with *Finnigan* instruments (type *LGC* or *TSQ 7000*) or *Bruker* spectrometers (types *Apex-Q IV 7T* and *micrOTOF API*). High-resolution spectra were obtained with the *Bruker Apex-Q IV 7T* or the *Bruker micrOTOF*, respectively. ^{1}H and ^{13}C NMR spectra were recorded with *Varian Unity 300*, *Varian Inova 600* spectrometers. Chemical shifts are given in parts per million (ppm) relative to TMS. Abbreviations for multiplicities are: s, singlet; d, doublet; t, triplet; m, multiplet. Coupling constants are given in Hertz; Hz. Flash chromatography was performed using *Merck* silica gel 60. Thin layer chromatography (TLC) was carried out using *Merck* aluminum plates of silica gel 60 F_{254}. HPLC purification was performed on a *JASCO* instrument (pump type PU-2080*plus*, UV/VIS-detector UV-875, online-deaerator PG-2080-53). UV-absorption was detected at 280 nm. Peptides were purified using a *LiChrospher* C18-RP-HPLC-column, 100 Å, 10 µm, 250 □ 20 mm with a flow rate of 8 mL/min, isocratic conditions 90 % MeOH / 10 % H_2O and 0.1 % trifluoroacetic acid (TFA). The fractions containing the desired product were collected and lyophilized. The peptides were automatically synthesized via SPPS using a peptide synthesizer (*ABI 433A*, *Applied Biosystems*) by applying the *FastMoc 0.1* mode. Following reagents, protocols and procedures were used for deprotection (20 % piperidine in NMP), coupling (HBTU [*O*-benzotriazole-*N*,*N*,*N*',*N*'-tetramethyluronium hexafluorophosphate] / HOBt [*N*-hydroxybenzotriazole] / DIEA [diisopropylethylamine] in NMP) and capping (Ac_2O / DIEA / HOBt / NMP).

Synthesis of amino acid building blocks

Scheme 1. Synthesis of amino acid building blocks serving as lipid-like residues for incorporation into the peptides backbone.

Synthesis of *N*-Fmoc-D-Ser(decanoyl)-OH (1). A solution of *N*-Fmoc-D-serine (95.0 mg, 290 µmol, 1.0 equiv.) in trifluoro acetic acid (TFA) (5 mL) was treated with decanoyl chloride (296 µL, 1.45 mmol, 5.0 equiv.) at 0 °C and stirred at room temperature for 1 h. The reaction was quenched with cold water (25 mL). The colorless precipitate was collected by filtration and washed with cold water. The crude product was purified by flash chromatography with ethyl acetate/pentane/acetic acid (75/25/0.5) as eluent. The product was obtained as a colorless solid (91.0 mg, 109 µmol, 65 %). TLC (ethyl acetate/pentane/acetic acid = 75/25/1, v/v/v) R_f = 0.46; ESI-MS: *m/z*: 504.3 $[M+Na]^+$, 984.9 $[2M+Na]^+$; HR-MS: *m/z*: calcd. For $C_{28}H_{35}NO_6$ $[M+H]^+$: 482.25371, found: 482.25371; ^{1}H-NMR ($CDCl_3$, 300 MHz, □ in ppm): 0.87 (t, $^{3}J_{H,H}$ = 7 Hz, 3 H, CH_3), 1.20-1.35 (m, 12 H, 3'-8'-$(CH_2)_6$), 1.53-1.66 (m, 2 H, 2'-CH_2), 2.33 (t, $^{3}J_{H,H}$ = 7 Hz, 2 H, 1'-CH_2), 4.24 (t, $^{3}J_{H,H}$ = 7 Hz, 1 H, Fmoc-CH), 4.43 (d, $^{3}J_{H,H}$ = 7 Hz, 2 H, Fmoc-CH_2), 4.49-4.57 (m, 2 H, *β*-CH_2), 4.65-4.72 (m, 1 H, *α*-CH), 5.59 (d, $^{3}J_{H,H}$ = 7 Hz, 1 H, NH), 7.26 (t, $^{3}J_{H,H}$ = 7 Hz, 2 H,

Fmoc-H3), 7.40 (t, $^{3}J_{H,H}$ = 7 Hz, 2 H, Fmoc-H4), 7.58 (d, $^{3}J_{H,H}$ = 6 Hz, 2 H, Fmoc-H2), 7.78 (d, $^{3}J_{H,H}$ = 7 Hz, 2 H, Fmoc-H5), 9.30 (s_{br}, 1 H, COOH); ^{13}C-NMR ($CDCl_3$,125 MHz, □ in ppm): □ = 14.1 (CH_3), 22.6 (CH_2), 24.7 (CH_2), 29.1 (CH_2), 29.2 (CH_2), 29.2 (CH_2), 29.4 (CH_2), 31.8 (2'-CH_2), 33.9 (1'-CH_2), 47.0 (Fmoc-CH), 53.3 (*α*-C), 63.6 (*β*-C), 67.5 (Fmoc-CH_2), 120.0 (Fmoc-C_4), 125.0 (Fmoc-C_1), 127.1 (Fmoc-C_2), 127.8 (Fmoc-C_3), 141.3 (Fmoc-C_{4a}), 143.6 (Fmoc-C_{8a}), 156.0 (Fmoc-CO), 173.5 (*C*OOR), 181.3 (*C*OOH).

Synthesis of *N*-Fmoc-D-Ser(undecanoyl)-OH (2)

N-Fmoc-D-Ser(undecanoyl)-OH **2** was prepared following the procedure described above for the synthesis of *N*-Fmoc-D-Ser(decanoyl)-OH **1**. The crude product was purified by flash chromatography with ethyl acetate/pentane/acetic acid (75/25/0.5) as eluent. The product was obtained as a colorless solid (88.0 mg, 178 µmol, 61 %). TLC (ethyl acetate/pentane/ acetic acid = 75/25/1, v/v/v) R_f = 0.42; ESI-MS: *m/z*: 518.3 $[M+Na]^+$, 1013.0 $[2M+Na]^+$; HR-MS: *m/z*: calcd. for $C_{29}H_{37}NO_6$ $[M+H]^+$: 496.26936, found: 496.26934; ^{1}H-NMR ($CDCl_3$, 300 MHz, □ in ppm): 0.89 (t, $^{3}J_{H,H}$ = 7 Hz, 3 H, CH_3), 1.19-1.35 (m, 14 H, 3'-9'-$(CH_2)_7$), 1.52-1.68 (m, 2 H, 2'-CH_2), 2.34 (t, $^{3}J_{H,H}$ = 7 Hz, 2 H, 1'-CH_2), 4.23 (t, $^{3}J_{H,H}$ = 7 Hz, 1 H, Fmoc-CH), 4.42 (d, $^{3}J_{H,H}$ = 7 Hz, 2 H, Fmoc-CH_2), 4.49-4.57 (m, 2 H, *β*-CH_2), 4.65-4.72 (m, 1 H, *α*-CH), 5.59 (d, $^{3}J_{H,H}$ = 7 Hz, 1 H, NH), 7.28 (t, $^{3}J_{H,H}$ = 7 Hz, 2 H, Fmoc-H3), 7.41 (t, $^{3}J_{H,H}$ = 7 Hz, 2 H, Fmoc-H4), 7.58 (d, $^{3}J_{H,H}$ = 6 Hz, 2 H, Fmoc-H2), 7.78 (d, $^{3}J_{H,H}$ = 7 Hz, 2 H, Fmoc-H5), 10.75 (s_{br}, 1 H, COOH). ^{13}C-NMR ($CDCl_3$,125 MHz, □ in ppm): 14.1 (CH_3), 22.6 (CH_2), 24.6 (CH_2), 24.8 (CH_2), 29.1 (CH_2), 29.2 (CH_2), 29.2 (CH_2), 29.4 (CH_2), 31.8 (2'-CH_2), 33.9 (1'-CH_2), 47.0 (Fmoc-CH), 53.3 (*α*-C), 63.6 (*β*-C), 67.5 (Fmoc-CH_2), 120.0 (Fmoc-C_4), 125.0 (Fmoc-C_1), 127.1 (Fmoc-C_2), 127.7 (Fmoc-C_3), 141.3 (Fmoc-C_{4a}), 143.6 (Fmoc-C_{8a}), 155.9 (Fmoc-CO), 174.2 (*C*OOR), 180.2 (*C*OOH).

Peptide synthesis

H(O)C-V-G-A-L-A-V-V-V-W-L-W-L-W-S(undecanoyl)-W-NHCH$_2$CH$_2$OH gA_1

R_1: $NHCH_2CH_2OH$, R_2: D-Ser(undecanoyl), R_3: D-Leu.Yield: 26 %; HPLC (isocratic conditions 85 % MeOH / 15 % H_2O and 0.1 % TFA): t_R = 27 min; ESI-MS: *m/z*: 2025.18 $[M+H]^+$, 1990.9 $[M+Na]^+$; HR-MS: *m/z*: calcd. for $C_{107}H_{154}N_{20}O_{19}$ $[M+2H]^{2+}$: 1012.59223, found: 1012.59142.

H(O)C-V-G-A-L-A-V-V-V-W-L-W-L-W-S(decanoyl)-W-OH gA_2

R_1: OH, R_2: D-Ser(decanoyl), R_3: D-Leu. Yield: 44 %; HPLC (isocratic conditions 90 % MeOH / 10 % H_2O and 0.1 % TFA): t_R = 38 min; ESI-MS: *m/z*: 1966.0 $[M-H]^-$, 1990.9 $[M+Na]^+$; HR-MS: *m/z*: calcd. for $C_{104}H_{147}N_{19}O_{19}$ $[M+2H]^{2+}$: 984.06253, found: 984.06331.

H(O)C-V-G-A-L-A-V-V-V-W-L-W-S(decanoyl)-W-S(decanoyl)-W-OH gA_3

R_1: OH, R_2 = R_3: D-Ser(decanoyl). Yield: 20 %; HPLC (isocratic conditions 90 % MeOH / 10 % H_2O and 0.1 % TFA): t_R = 24 min; ESI-MS: *m/z*: 2096.22 $[M+H]^+$, 1990.9 $[M+Na]^+$; HR-MS: *m/z*: calcd. for $C_{111}H_{159}N_{19}O_{21}$ $[M+2H]^{2+}$: 1048.10517, found: 1048.10464.

H(O)C-V-G-A-L-A-V-V-V-W-L-W-L-W-S(decanoyl)-W-S(decanoyl)-OH gA_4

R_1: D-Ser(decanoyl)-OH, R_2: D-Ser(decanoyl), R_3: D-Leu. Yield: 13 %; HPLC (isocratic conditions 90 % MeOH / 10 % H_2O and 0.1 % TFA): t_R = 22 min; ESI-MS: *m/z*: 2209.21 $[M+H]^+$, 1990.9 $[M+Na]^+$; HR-MS: *m/z*: calcd. for $C_{117}H_{170}N_{20}O_{22}$ $[M+2H]^{2+}$: 1105.10689, found: 1105.10689.

The synthesis for compounds **gA_2** , **gA_3** and **gA_4** was performed on Fmoc-L-Trp(Boc)-wang resin (0.60 mmol/g resin loading capacity) (GL Biochem Ltd.). For the peptide **gA_1**, the synthesis was carried out on glycinol 2-chlorotrityl-resin (0.50 mmol/g). The loading with the first amino acid (Fmoc-L-Trp(Boc)-OH) was carried out manually in a syringe equipped with a PE-frit; the resin was pre-swollen in NMP for 2 h. PyBOP (5 equiv.) was added to a solution of the amino acid derivative (5 equiv.), DIEA (10 equiv.) and HOBt (5 equiv.) in NMP (2 mL) and kept at room temperature for 5 min. The resulting suspension was added to the resin and the reaction mixture was shaken in the syringe at room temperature for 1 h. After washing the resin with NMP (3 x 3 min), DCM (2 x 3 min) and NMP (3 x 3 min), the loading procedure was repeated. After the washing protocol the resin was dried over KOH in a desiccator. All peptide syntheses were performed via SPPS using a peptide synthesizer (*ABI 433A, Applied Biosystems*). Double coupling was performed for all amino acids using HOBt/HBTU/DIEA in NMP for 40 min. After the automated syntheses, the resin was placed in a syringe equipped with a PE-frit and dried over KOH in a desiccator. The formylation of the peptides with pentafluorophenyl formate **3** (1 mL, 14 mM) was carried out on resin. All peptides were cleaved from the resin using a TFA/EDT/thioaniosole/TIS/H_2O (85/5/5/2.5/2.5) solution (1.0 mL – 2 mL/100 mg resin) at room temperature for 90 min. All solvents were evaporated and the crude product was precipitated with cold diethyl ether (5 mL) and purified by reverse phase HPLC (isocratic conditions 90 % MeOH / 10 % H_2O and 0.1 % TFA).

Preparation of peptide/lipid complexes for circular dichroism spectroscopy. Large unilamellar vesicles of 1,2-dimyristoyl-*sn*-glycero-3-phosphocholine (DMPC) were

prepared according to the method described by MacDonald et al.(18) For CD spectroscopy, DMPC was dissolved in TFE (10 mg/mL) and the peptides were dissolved also in TFE and mixed. Concentrations of peptide stocks were determined by UV absorption. Removing the solvents in a nitrogen stream at temperatures above the lipid main phase transition temperature of DMPC (t_m = 23.6 °C)(19) produced an almost clear lipid/peptide film at the test tube walls. After removing of residual solvent under reduced pressure for 12 h at $T > t_m$, the lipid films were rehydrated with ultra pure water. After 1 h of incubation at $T > t_m$, the hydrated lipid films were vortexed several times for 30 s with subsequent incubation for 5 min (5 cycles). The milky suspensions were extruded 31 times through a polycarbonate membrane (100 nm nominal pore size) using a miniextruder (Liposofast, Avestin, Ottawa, Canada) to produce an almost clear vesicle suspension. Subsequently, the vesicle suspensions were deposited in precision cells (Quartz Suprasil, Hellma, Mühlheim, Germany) and used for CD spectroscopy.

Water and ion permeation measurements

Preparation of black lipid membrane for ion and water flux measurements

We formed solvent free membranes (20) from 1,2-diphytanoyl-*sn*- glycerol-3-phosphocholine (DiPhyPC) (Avanti Polar Lipids, Alabaster, AL) dissolved in n-hexane (20 mg/ml). First we spread the solution onto the air-water interface of the chamber separated in two halves by a septum with an aperture between 150 and 180 µm. Raising the buffer level above the aperture resulted in folding of the monolayers into a bilayer. We added gramicidin A or its derivatives from an ethanol stock solution to both sides of the black lipid membrane (BLM).

Buffer Solutions

For scanning electrochemical microscopy experiments the buffer consisted of 150 mM choline chloride (ChCl) (Fluka), 1 mM potassium chloride (KCl) (Fluka), 200 µM magnesium chloride ($MgCl_2$) (Sigma chemical co., St. Louis) and 20 mM Tris(hydroxymethyl)aminomethane (Tris) (Sigma chemical co.). We adjusted pH to 8.4 and stirred both compartments during the measurement with small magnetic rods. For single channel current measurements we increased the KCl concentration to 100 mM.

Water flux measurements

To determine the concentration of the impermeant ion Mg^{+2} we fabricated Mg^{2+} sensitive microelectrodes by pulling Borosilicate capillaries (GB150F-10, Science Products GmbH, Hofheim) to a tip diameter of 1-3 µm with a pipette puller (model PP83, Narishige, Tokyo, Japan). After silanization with Bis(dimethylamino)-dimethylsilane (Fluka) we filled the tip with a magnesium sensitive cocktail (Magnesium Ionophore II – Cocktail A, Fluka, Sigma-Aldrich).

For measuring $c_i(x)$, we connected both the Mg^{2+} sensitive electrode and the Ag/AgCl reference electrode to an electrometer (Model 6514, Keithley Instruments, Cleveland, Ohio) and immersed them into the trans-compartment. A hydraulic step motor (Model PC-5N, Narishige, Tokjo, Japan) moved the microelectrode perpendicular to the membrane plane with a velocity of 2 µm/s. When moving the electrode in the opposite direction no hysteresis occurred, indicating the lack of artifacts due to electrode movement. A spontaneous jump of the electrode potential indicated the position of the membrane.

Measurements of transmembrane current and membrane conductance

We determined the conductance of the membrane before and after the water flux measurement. Therefore a function generator (model 33120A, Agilent Technologies, Santa Clara, United States) applied rectangle voltage pulses at 300 Hz via chlorinated silver electrodes to the membrane. The access resistance of the electrodes was below 10 kΩ, and therefore at least one order of magnitude below the membrane resistance, which did not drop below 200 kΩ. To avoid an apparent increase of membrane resistance due to electrolyte polarization in the electrical field we performed the measurements in an alternating current circuit. We amplified the output signal (npi VA-10x) and a digital oscilloscope (model TDS 210, Tektronix, Beaverton, United States) displayed the output and input signal.

Single channel conductivity

Under voltage clamp conditions a patch clamp amplifier (EPC-10, HEKA Elektronik Dr. Schulze GmbH Lambrecht/Pfalz, Germany) measured the transmembrane current (see Fig. PP4). The recording filter was a 4-pole Bessel with a 3-db corner frequency of 0.1 kHz. The acquired raw data were analyzed with the help of the TAC software package (Bruxton Corporation, Seattle, WA). Gaussian filters between 10 and 20 Hz were applied to reduce noise. From the current versus potential curves we determined the single channel conductances. The associated errors were derived from the propagation of the statistical error associated with each current measurement.

Supplementary methods bibliography

1. Hess, B., C. Kutzner, D. van der Spoel, and E. Lindahl. 2008. GROMACS 4: Algorithms for Highly Efficient, Load-Balanced, and Scalable Molecular Simulation. J. Chem. Theory Comput. 4:435-447.
2. Darden, T., D. York, and L. Pedersen. 1993. Particle mesh Ewald: an Nlog(N) method for Ewald sums in large systems. J. Chem. Phys. 98:10089-10092.
3. Miyamoto, S., and P. A. Kollman. 1992. SETTLE: An Analytical Version of the SHAKE and RATTLE Algorithms for Rigid Water Models. J. Comput. Chem. 13:952-962.
4. Hess, B. 2008. P-LINCS: A Parallel Linear Constraint Solver for Molecular Simulation. J. Chem. Theory Comput. 4:116-122.
5. Bussi, G., D. Donadio, and M. Parrinello. 2007. Canonical sampling through velocity rescaling. J. Chem. Phys. 126:014101.
6. Berendsen, H. J. C., J. P. M. Postma, A. DiNola, and J. R. Haak. 1984. Molecular dynamics with coupling to an external bath. J. Chem. Phys. 81:3684-3690.
7. Cieplak, P., W. D. Cornell, C. Bayly, and P. A. Kollman. 1995. Application of the multimolecule and multiconformational RESP methodology to biopolymers: Charge derivation for DNA, RNA, and proteins. J. Comput. Chem. 16:1357-1377.
8. Wang, J., R. M. Wolf, J. W. Caldwell, P. A. Kollman, and D. A. Case. 2004. Development and testing of a general amber force field. J. Comput. Chem. 25:1157-1174.

9. Berger, O., O. Edholm, and F. Jahnig. 1997. Molecular dynamics simulations of a fluid bilayer of dipalmitoylphosphatidylcholine at full hydration, constant pressure, and constant temperature. Biophysical Journal 72:2002-2013.
10. Cordomí, A., G. Caltabiano, and L. Pardo. 2012. Membrane Protein Simulations Using AMBER Force Field and Berger Lipid Parameters. J. Chem. Theory Comput. 8:948-958.
11. Berendsen, H. J. C., J. R. Grigera, and T. P. Straatsma. 1987. The missing term in effective pair potentials. The Journal of Physical Chemistry 91:6269-6271.
12. Joung, I. S., and T. E. Cheatham. 2008. Determination of alkali and halide monovalent ion parameters for use in explicitly solvated biomolecular simulations. The Journal of Physical Chemistry B 112:9020-9041.
13. de Groot, B. L., D. P. Tieleman, P. Pohl, and H. Grubmüller. 2002. Water permeation through gramicidin A: desformylation and the double helix; a molecular dynamics study. Biophys J. 82:2934-2942.
14. Portella, G., P. Pohl, and B. L. de Groot. 2007. Invariance of single-file water mobility in gramicidin-like peptidic pores as function of pore length. Biophys. J. 92:3930-3937.
15. de Groot, B. L., and H. Grubmüller. 2005. The dynamics and energetics of water permeation and proton exclusion in aquaporins. Curr. Opin. Struct. Biol. 15:176-183.
16. Espinosa, E., E. Molins, and C. Lecomte. 1998. Hydrogen bond strengths revealed by topological analyses of experimentally observed electron densities. Chem. Phys. Lett. 285:170-173.
17. C. J. Stankovic, J. M. Delfino, and S. L. Schreiber. 1990. Anal. Biochem 184:100-103.
18. R. C. MacDonald, R. I. MacDonald, B. P. M. Menco, K. Takeshita, N. K. Subbarao, and L. Hu. 1991. Biochim. Biophys. Acta 1061:297-303.
19. S. G. Boxer. 2000. Current Opinion in Chemical Biology 4:704-709.
20. Montal, M., and P. Mueller. 1972. Formation of bimolecular membranes from lipid monolayers and a study of their electrical properties. Proc. Natl. Acad. Sci. U. S. A. 69:3561-3566.